Hindawi
Analytical Cellular Pathology
Volume 2023, Article ID 6660072, 11 pages
https://doi.org/10.1155/2023/6660072

Research Article

MicroRNA-17-5p and MicroRNA-130b-3p Promote Radioresistance of Glioma Stem Cells by Targeting PTEN/AKT/HIF-1α Pathway-Controlled Phosphopentose Metabolism

Tao Xie,[1] Yu-Hao Ding,[1] Jun Dong,[2] and Xi-An Fu[1]

[1]*Department of Neurosurgery, The Affiliated Suzhou Hospital of Nanjing Medical University, Suzhou Municipal Hospital, Gusu School, Nanjing Medical University, 215008, Suzhou, Jiangsu Province, China*
[2]*The Experimental Center and Department of Neurosurgery, The Second Affiliated Hospital of Soochow University, 215004, Suzhou, Jiangsu Province, China*

Correspondence should be addressed to Jun Dong; dongjun@suda.edu.cn and Xi-An Fu; xianfu@njmu.edu.cn

Received 15 January 2023; Revised 21 May 2023; Accepted 20 July 2023; Published 4 August 2023

Academic Editor: Elena Andreucci

Background. The radioresistance of glioma stem cells (GSCs) is related to some microRNAs (miRs) generated by radiation. This study aimed to investigate the effects of miR-17-5p and miR-130b-3p on the radiosensitivity of GSCs. *Methods*. miR-17-5p and miR-130b-3p expressions in SU3 and SU3-5R cells were determined. SU3 cells transfected with miR-17-5p or miR-130b-3p mimics or inhibitors were used to determine cell viability after irradiation as well as to examine changes of supernatant glucose, intracellular glucose 6-phosphate dehydrogenase (G6PDH), 6-phosphogluconate dehydrogenase (6-PGDH), reduced nicotinamide adenine dinucleotide phosphate (NADPH), reduced glutathione (GSH), glutathione peroxidase (GSH-Px), phosphatase and tensin homolog (PTEN), hypoxia-inducible factor-1α (HIF-1α), glucose transporter (GLUT)-1/3, protein kinase B (AKT), and p-AKT levels. The target gene of the two miRs was verified by luciferase reporter gene assay. *Results*. miR-17-5p and miR-130b-3p expressions in the radiation-resistant SU3-5R cells or 8 Gy irradiation-treated SU3 cells were high. After transfection of SU3 cells with miR-17-5p or miR-130b-3p mimics, cell viability, intracellular HIF-1α, GLUT-1/3, AKT, and p-AKT protein expressions, and intracellular G6PDH, 6-PGDH, NADPH, GSH-Px, and GSH levels were high, whereas intracellular PTEN expression and supernatant glucose were low. The opposite effects were also observed in the two miR inhibitors-transfected SU3 cells. Further study confirmed that miR-17-5p or miR-130b-3p could directly bind with the PTEN. *Conclusion*. Radiation-induced miR-17-5p and miR-130b-3p might cause the radioresistance of GSCs, and the mechanisms were associated with the enhancement of antioxidant production, which was from the increments of AKT/HIF-1α signaling pathway-controlled glucose transmembrane transport and phosphopentose metabolism by targeting PTEN.

1. Introduction

Glioma is a primary intracranial tumor with infiltrating growth, and the tumor is generally treated with surgery and postoperative radio/chemotherapy. The adjuvant therapy of the latter aims to kill the remaining tumor cells after surgery. However, the effect of radiotherapy fails to meet patients' expectations due to the presence of glioma stem cells (GSCs) [1–3]. Therefore, GSCs have become a hot research field to discover new potential targets for glioma treatment [4].

Literature data have shown that some microRNAs (miRs) were involved in radiosensitivity changes of glioma cells [5, 6]. After the glioma being irradiated, the expressions of some miRs in tumor tissues increased, and overexpressions of these miRs could induce the radioresistance [7]. Similarly, after GSCs were irradiated, some miRs, such as miR-19a-3p, miR-19b-3p, and miR-21-5p, also exhibited high expressions [8] and could facilitate the abnormal glucose metabolism, proliferation, and repair of tumor cells [9]. Thus, miRs caused

by radiation may be one of the important mechanisms underlying radioresistance.

We used the human GSC strain SU3 and its radiation-resistant cell strain SU3-5R to explore the differences in some miR expressions and observed that the expressions of miR-17-5p and miR-130b-3p were higher in the SU3-5R cells than in the SU3 cells, thus assuming that both miRs might be involved in radioresistance of glioma. As is known, the role of miR-17-5p in tumors is mainly manifested in the biological effect of oncogene [10], and its high expression in glioma tissues may be predicted to have a poor prognosis [11], but disputes have arisen about its effect on radiosensitivity [12, 13]. miR-130b-3p expression varies in different tumors, and its biological effect can be manifested in the duality of cancer suppression and carcinogenesis. Some scholars have observed that miR-130b was correlated to the chemotherapy sensitivity of glioma [14], but the relationship between miR-130b and glioma's radiosensitivity has not been reported yet. In this work, we wanted to use miR-17-5p or miR-130b-3p mimics- or inhibitors-transfected SU3 cells to explore the effects of both miRs on the radiosensitivity of GSCs and to provide new targets for the development of radiosensitizers.

2. Materials and Methods

2.1. Materials. Human GSC strain SU3, derived from a fresh surgical specimen of a highly aggressive glioblastoma multiforme, was obtained from subculture and monoclone *in vitro* and had a high expression of the stem cell marker protein CD133 [15]. Human GSC strain SU3-5R is a radiation-resistant cell strain that was formed after being irradiated for five times [16]. Both cell strains were supplied by the Department of Neurosurgery of the Second Affiliated Hospital of Soochow University (Suzhou, China). Dulbecco modified Eagle medium (DMEM) high-glucose medium was obtained from HyClone Company (Logan, UT, USA). All-in-one RT MasterMix, EvaGreen 2× quantitative polymerase chain reaction (qPCR) MasterMix-Low ROX, miRNA cDNA synthesis kit, EvaGreen miRNA qPCR MasterMix, and luciferase assay kit were bought from Applied Biological Materials Inc. (Vancouver, Canada). 3-(4,5 dimethylthiazol-2-yl)-2, 5-diphenyltetrazolium bromide (methyl thiazolyl tetrazolium, MTT) was acquired from Sigma–Aldrich Company (St. Louis, MO, USA). Antihypoxia-inducible factor-1α (HIF-1α) antibody was supplied by Abcam (Cambridge, UK). Antiglucose transporter-1 (GLUT-1), GLUT-3, and homologous phosphatase and tensin homolog (PTEN) antibodies were obtained from Affinity Company (Golden, USA). Antiprotein kinase B (AKT), p-AKT, and β-actin antibodies were bought from Cell Signaling Technology (Danvers, MA, USA). Trizol reagent was supplied by Sangon Gene Company (Shanghai, China). PCR primers were designed and synthesized by Sangon Gene Company (Shanghai, China), their sequences were shown in *Supplementary 1*, the internal reference primer U6 used for miR determination was a secret concerning product of the company. miR-17-5p mimic or inhibitor, miR-130b-3p mimic or inhibitor, and their mimic negative control (NC) and inhibitor NC were designed and synthesized by Shanghai Biotend Biotechnology Co., Ltd. (Shanghai, China). pSV-β-galactosidase control vector was provided by Promega (Madison, WI, USA). Lipofectamine 2000 transfection reagent was supplied by Life Technologies (Carlsbad, CA, USA). Plenti-UTR-Luc-Blank vector, PTEN-WT 3′-UTR Plenti-reporter-Luciferase vector, PTEN-MUT 3′-UTR Plenti-reporter-Luciferase vector, and luciferase assay kit were acquired from Applied Biological Materials Inc. (Vancouver, Canada). Assay kits of glucose 6-phosphate dehydrogenase (G6PDH), 6-phosphogluconate dehydrogenase (6-PGDH), and reduced nicotinamide adenine dinucleotide phosphate (NADPH) were obtained from Suzhou Keming Biotechnology Co., Ltd. (Suzhou, China). Assay kits of glucose, reduced glutathione (GSH), glutathione reductase (GR), and glutathione peroxidase (GSH-Px) were provided by Nanjing Jiancheng Bioengineering Institute (Nanjing, China). Chemiluminescence analyzer was supplied by Thermo Fisher Scientific (China) Co., Ltd., and UV-2600 spectrophotometer was obtained from SHIMADZU, Japan. ABI7500 fluorescent quantitative PCR instrument was supplied by American Thermo Company, Tecan Infinite M1000 Pro full-wavelength multifunctional microplate reader was bought from the Swiss company TECAN, and RS-2000Pro biological X-ray irradiator was obtained from Rad Source, USA.

2.2. Comparisons of miR-17-5p and miR-130b-3p Expressions in SU3 and SU3-5R Cells. After the cell density was adjusted to 6×10^5/mL, both cells were, respectively, inoculated in a six-well culture plate with 2 mL each well and cultured in DMEM high-glucose medium containing 10% fetal bovine serum for 24 hr. The cells were then collected, and the expression levels of intracellular miR-17-5p and miR-130b-3p were determined by the real-time fluorescent quantitative PCR method [17].

2.3. The Effect of Different Irradiation Doses on SU3 Cell Proliferation. In brief, 1×10^5 cells/well were inoculated in a 96-well plate with 150 μL each well and then cultured in an incubator for 24 hr. When the monolayer in the bottom of the well reached approximately 85%, the cells were divided into the control group and the irradiation 8, 10, and 15 Gy groups. At 0, 6, 12, and 24 hr after exposure to X-ray irradiation, cell survival rate was examined using the MTT method [17].

2.4. The Effects of Irradiation on miR-17-5p and miR-130b-3p Expressions in SU3 Cells. SU3 cells were inoculated with 6×10^5/ mL density into a six-well culture plate. When the cells reached 85% confluence, they were divided into the control and irradiation groups. The irradiation dose of the latter was 8 Gy with dose rate of 1.5 Gy/min. The cells were collected at 6, 12, and 24 hr after irradiation, and the expressions of intracellular miR-17-5p and miR-130b-3p were determined [17].

2.5. Radiosensitivity Determination of miR-17-5p or miR-130b-3p Mimics- or Inhibitors-Transfected SU3 Cells. SU3 cells were classified into the control group, radiation group, mimic NC group, miR-17-5p mimic group, miR-130b-3p mimic group, inhibitor NC group, miR-17-5p inhibitor group, and miR-130b-3p inhibitor group. First, SU3 cells were transfected with miR mimics, miR inhibitors, or NC

miRs for 24 hr under optimal transfection conditions, and the cells of the latter seven groups were then irradiated with an irradiation dose of 10 Gy. Cell viability was analyzed at 0, 12, and 24 hr after irradiation.

2.6. Changes in the Glucose Transmembrane Transport, Phosphopentose Metabolism, and Related Protein Expressions in miR-17-5p or miR-130b-3p Mimics- or Inhibitors-Transfected SU3 Cells. SU3 cells were classified into seven groups: control group, mimic NC group, miR-17-5p mimic group, miR-130b-3p mimic group, inhibitor NC group, miR-17-5p inhibitor group, and miR-130b-3p inhibitor group. First, SU3 cells were transfected with miR mimics, miR inhibitors, or NC miRs for 24 hr, and then incubated with the fresh DMEM low-glucose medium (to determine the glucose content in the culture supernatant) or DMEM high-glucose medium (to determine other indicators) for 12 hr. Finally, the culture supernatant and cells were respectively collected, the contents of supernatant glucose and intracellular G6PDH, 6-PGDH, NADPH, GSH, GR, and GSH-Px were measured in accordance with the operation methods provided by the suppliers, and the expressions of intracellular HIF-1α, GLUT-1, GLUT-3, PTEN, AKT, and p-AKT proteins were determined by the Western blot method [17].

2.7. The Test of Targeted Binding of miR-17-5p or miR-130b-3p with PTEN. Bioinformatics predicted that PTEN might be a common target gene of miR-17-5p and miR-130b-3p (*Supplementary 2*). The plasmids of Plenti-3′-UTR-Blank, PTEN-3′-UTR-WT, PTEN-3′-UTR-MUT, and pSV-β-Galactosidase Control Vector were prepared in accordance with the product instructions, and SU3 cells were then classified into the Plenti-3′-UTR-Blank + miR mimic NC + pSV-β-Galactosidase Control Vector cotransfection group, Plenti-3′-UTR-Blank + miR-17-5p (or miR-130b-3p) mimic + pSV-β-Galactosidase Control Vector cotransfection group, PTEN-3′-UTR-WT + miR mimic NC + pSV-β-Galactosidase Control Vector cotransfection group, PTEN-3′-UTR-WT + miR-17-5p (or miR-130b-3p) mimic + pSV-β-Galactosidase Control Vector cotransfection group, PTEN-3′-UTR-MUT + miR mimic NC + pSV-β-Galactosidase Control Vector cotransfection group, and PTEN-3′-UTR-MUT + miR-17-5p (or miR-130b-3p) mimic + pSV-β-Galactosidase Control Vector cotransfection group. After the plasmids were cotransfected for 48 hr in accordance with the requirement of each group, the luciferase assay kit and β-galactosidase reporter gene activity detection kit were used to respectively determine the fluorescence value at 560 nm and absorbance value at 420 nm, which might indicate the luciferase activity and β-galactosidase reporter gene activity, respectively. The latter acted as an internal normalization.

2.8. Statistical Analysis. Experimental data were expressed as mean ± SD. SPSS 20.0 statistical analysis software was used for data processing. Single-factor or two-factor variance analysis was applied to analyze significant differences between groups. $P<0.05$ was considered to be of statistical significance.

3. Results

3.1. The Effect of Irradiation on the Viability of SU3 Cells. Compared with the control group, cell viability was significantly reduced when the irradiation dose was 10 Gy or more (*Supplementary 3*, $P<0.05$ or $P<0.01$) but was not significantly affected within 24 hr after exposure to 8 Gy irradiation (*Supplementary 3*). These results suggested that the maximum tolerable radiation dose of SU3 cells is 8 Gy, and the minimum effective radiation dose is 10 Gy.

3.2. Expressions of miR-17-5p and miR-130b-3p in SU3 and SU3-5R Cells. Compared with the SU3 cells, the expressions of miR-17-5p and miR-130b-3p in radiation-resistant SU3-5R cells significantly increased (*Supplementary 4*, $P<0.01$). After treatment of SU3 cells with 8 Gy irradiation, the expressions of both miRs significantly increased at 12 and 24 hr after irradiation (*Supplementary 4*, $P<0.05$ or $P<0.01$). These results indicated that irradiation can induce the expressions of miR-17-5p and miR-130b-3p in SU3 cells; both miRs may be related to the formation of radioresistance.

3.3. miR-17-5p and miR-130b-3p Reduce Radiosensitivity of SU3 Cells. Figure 1 shows the result of cell viability of miR-17-5p or miR-130b-3p mimics- or inhibitors-transfected SU3 cells at 0, 12, and 24 hr after 10 Gy irradiation. Compared with the control group, the viability of SU3 cells in the 10 Gy irradiation group significantly decreased at 0, 12, and 24 hr after irradiation (Figure 1, $P<0.05$ or $P<0.01$). No significant difference in cell viability was observed between the 10 Gy irradiation group and the 10 Gy + mimic NC group or the 10 Gy + inhibitor NC group. Compared with the 10 Gy + mimic NC group, the viability of SU3 cells in the miR-17-5p or miR-130b-3p mimics-transfected groups increased significantly at 12 and 24 hr after irradiation (Figure 1, $P<0.05$). On the contrary, the viability of SU3 cells in the miR-17-5p or miR-130b-3p inhibitors-transfected groups decreased significantly at 12 and 24 hr after irradiation (Figure 1, $P<0.05$). These results confirmed that miR-17-5p or miR-130b-3p can reduce the radiosensitivity of SU3 cells.

3.4. miR-17-5p and miR-130b-3p Increase Glucose Transmembrane Transport and Phosphopentose Metabolism of SU3 Cells. Figure 2 showed that the levels of supernatant glucose and intracellular GLUT-1/3 protein expressions in the mimic NC group or inhibitor NC group were not significantly different from those of the control group. Compared with the mimic NC group, the content of supernatant glucose in the miR-17-5p or miR-130b-3p mimics-transfected groups was lower (Figure 2(a), $P<0.05$), whereas the expressions of intracellular GLUT-1/3 proteins were higher (Figures 2(b) and 2(c), $P<0.05$). On the contrary, after SU3 cells were transfected with miR-17-5p or miR-130b-3p inhibitors, the content of supernatant glucose increased significantly (Figure 2(a), $P<0.05$), whereas the expressions of intracellular GLUT-1/3 proteins decreased significantly (Figures 2(b) and 2(c), $P<0.05$). These results indicated

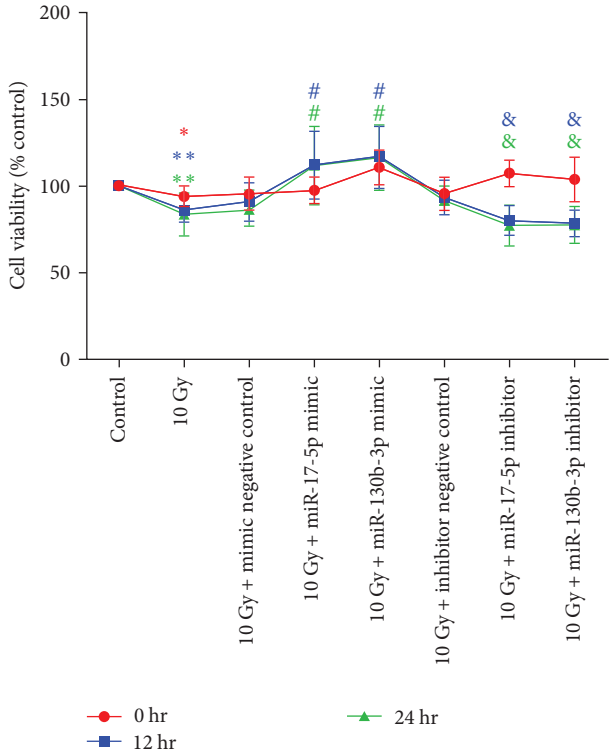

Figure 1: Cell viability at 0, 12, and 24 hr after exposure of miR-17-5p or miR-130b-3p mimics- or inhibitors-transfected SU3 cells to 10 Gy irradiation. The time of transfection with miR mimics, miR inhibitors, or NC miRs was 24 hr. Data were presented as mean ± SD of six independent experiments. $^{*}P<0.05$, $^{**}P<0.01$ vs. the control group at 0 (red), 12 (blue), and 24 hr (green) after irradiation; $^{\#}P<0.05$ vs. the 10 Gy + Mimic negative control group at 12 (blue) and 24 hr (green) after irradiation; $^{\&}P<0.05$ vs. the 10 Gy + Inhibitor negative control group at 12 (blue) and 24 hr (green) after irradiation. There was no obvious difference between the 10 Gy group and the 10 Gy + mimic negative control group or the 10 Gy + inhibitor negative control group.

that miR-17-5p or miR-130b-3p can enhance the glucose transmembrane transport of SU3 cells.

Figure 3 shows the effect of miR-17-5p or miR-130b-3p on phosphopentose metabolism in SU3 cells. The contents of intracellular G6PDH, 6-PGDH, and NADPH in the mimic NC group or inhibitor NC group were not significantly different from those of the control group. After SU3 cells were transfected with miR-17-5p or miR-130b-3p mimics, the contents of intracellular G6PDH, 6-PGDH, and NADPH increased significantly compared with those of the mimic NC group (Figure 3(a)–3(c), $P<0.05$ or $P<0.01$). On the contrary, after SU3 cells were transfected with miR-17-5p or miR-130b-3p inhibitors, the three indexes decreased significantly compared with those of the inhibitor NC group (Figure 3(a)–3(c), $P<0.05$ or $P<0.01$). These results indicated that miR-17-5p or miR-130b-3p can enhance the phosphopentose metabolism in SU3 cells.

Figure 4 shows the effects of miR-17-5p or miR-130b-3p on the antioxidant indexes in SU3 cells. The levels of intracellular GSH, GSH-Px, and GR in the mimic NC group or inhibitor NC group were not significantly different from those of the control group. After SU3 cells were transfected with miR-17-5p or miR-130b-3p mimics, the former both indexes increased significantly compared with those of the mimic NC group (Figures 4(a) and 4(b), $P<0.05$). On the contrary, after SU3 cells were transfected with miR-17-5p or miR-130b-3p inhibitors, the former both indexes decreased significantly compared with those of the inhibitor NC group (Figures 4(a) and 4(b), $P<0.05$). Meanwhile, the intracellular GR level did not show significant differences among the seven groups (Figure 4(c)). These results indicated that miR-17-5p and miR-130b-3p can increase the antioxidant capacity of SU3 cells and further proved that miR-17-5p or miR-130b-3p can enhance the phosphopentose metabolism in SU3 cells.

3.5. The Effects of miR-17-5p and miR-130b-3p on Expressions of PTEN mRNA and Related Proteins in SU3 Cells. Figure 5 showed that the expression levels of PTEN, AKT, p-AKT, and HIF-1α mRNA and/or proteins in the mimic NC group or inhibitor NC group were not significantly different from those of the control group. Compared with the mimic NC group, the expression levels of PTEN mRNA and protein significantly decreased in the cells transfected with miR-17-5p or miR-130b-3p mimics (Figures 5(a) and 5(b), $P<0.05$), whereas the expression levels of intracellular AKT, p-AKT, and HIF-1α proteins increased significantly (Figure 5(c)–5(e), $P<0.05$). Conversely, after SU3 cells were transfected with miR-17-5p or miR-130b-3p inhibitors, the expression levels of PTEN mRNA and protein increased significantly (Figures 5(a) and 5(b), $P<0.05$), whereas the expression levels of intracellular AKT, p-AKT, and HIF-1α proteins decreased significantly (Figure 5(c)–5(e), $P<0.05$). These results indicated that miR-17-5p or miR-130b-3p can increase the expressions of AKT and HIF-1α proteins by inhibiting the PTEN expression in SU3 cells.

3.6. Targeted Binding of miR-17-5p or miR-130b-3p with PTEN. According to the predictions from the miR target gene databases miRBase and TargetScan, PTEN is a potential target gene of miR-17-5p and miR-130b-3p. The regions where the two miRs bind with PTEN 3′ noncoding region are shown in *Supplementary 2*. Figure 6 shows the experimental results of luciferase reporter gene detection. After miR-17-5p mimic or miR-130b-3p mimic and the target gene PTEN 3′ noncoding region wild-type plasmid or mutant plasmid were cotransfected in SU3 cells, the luciferase activity of PTEN 3′ noncoding region wild-type plasmid group significantly decreased (Figure 6, $P<0.05$), whereas that of PTEN 3′ noncoding region mutant plasmid group did not change significantly. These results confirmed that miR-17-5p or miR-130b-3p can directly bind with the PTEN.

4. Discussion

In the present study, we found that miR-17-5p and miR-130b-3p expressions in radiation-resistant SU3-5R cells were significantly higher than those in ordinary SU3 cells. After SU3 cells were irradiated, miR-17-5p and miR-130b-3p

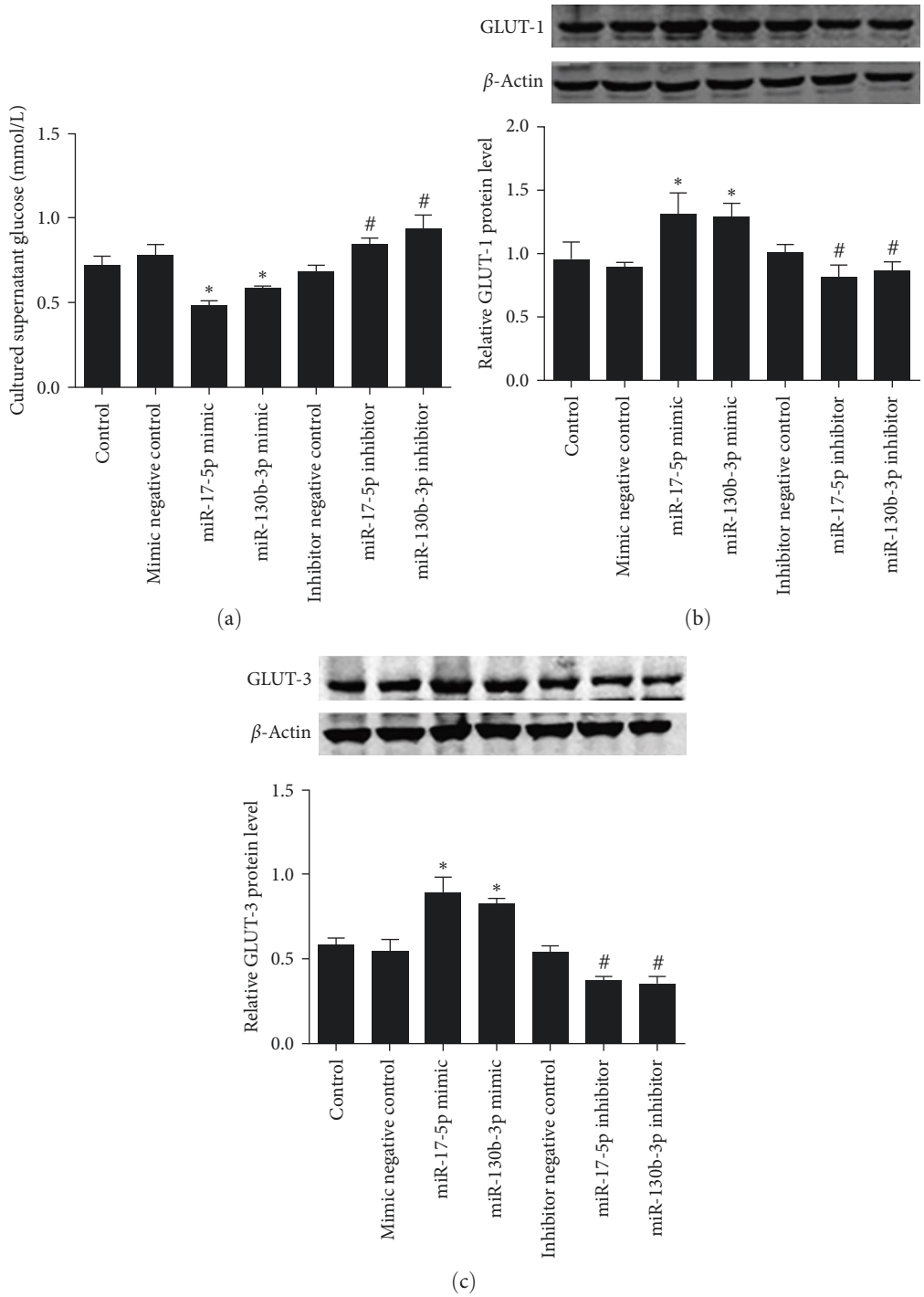

FIGURE 2: Supernatant glucose content and intracellular GLUT-1/3 protein expressions after transfection of SU3 cells with miR-17-5p or miR-130b-3p mimics or inhibitors for 36 hr. Data were presented as mean ± SD of three independent experiments. $^{*}P<0.05$ vs. the mimic negative control group; $^{\#}P<0.05$ vs. the inhibitor negative control group.

expressions also increased. These results suggested that the radiation-induced miR-17-5p and miR-130b-3p may be involved in the radioresistant formation of GSCs. To further investigate the effect of miR-17-5p and miR-130b-3p on the radiosensitivity of SU3 cells, their mimics and inhibitors were used in this study. The results showed that miR-17-5p or miR-130b-3p mimics-transfected SU3 cells could tolerate the minimum effective irradiation dose of 10 Gy, and cell viability increased remarkably after irradiation. Conversely, after transfection of SU3 cells with miR-17-5p or miR-130b-3p inhibitors, cell viability decreased substantially after 10 Gy irradiation. These results further suggested that the two miRs were involved

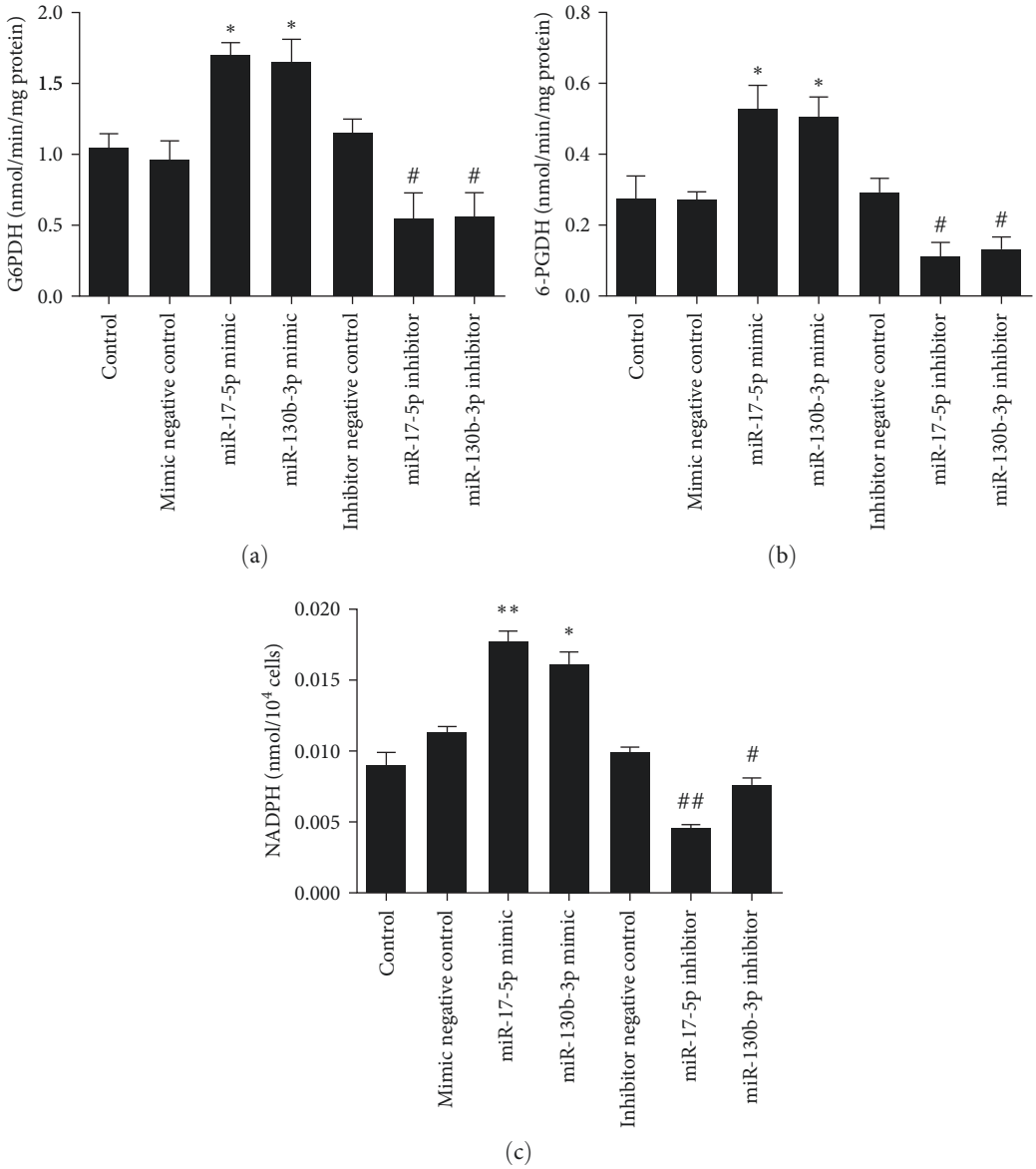

Figure 3: Intracellular G6PDH, 6-PGDH, and NADPH levels after transfection of SU3 cells with miR-17-5p or miR-130b-3p mimics or inhibitors for 36 hr. Data were presented as mean ± SD of three independent experiments. $^{*}P<0.05$, $^{**}P<0.01$ vs. the mimic negative control group; $^{\#}P<0.05$, $^{\#\#}P<0.01$ vs. the inhibitor negative control group.

in the radioresistance of GSCs. However, we did not investigate the relationship between miR-17-5p and miR-130b-3p in this study, which is a limitation and needs further research in the future.

HIF-1α can mediate the remodeling of carbohydrate metabolism of tumor cells, including an increase in glucose transmembrane transport and phosphopentose metabolism by regulating the expressions of GLUT-1/3 [18, 19] and activities of G6PDH and 6-PGDH [20, 21], which may finally facilitate the formation of radioresistance [22, 23]. Our present results showed that in SU3 cells transfected with miR-17-5p or miR-130b-3p mimics, the expressions of GLUT-1/3 proteins and activities of G6PDH and 6-PGDH increased substantially with the HIF-1α protein expression, whereas the content of supernatant glucose decreased substantially. The opposite results could also be observed in SU3 cells transfected with miR-17-5p or miR-130b-3p inhibitors. These results suggested that miR-17-5p and miR-130b-3p can increase the HIF-1α-controlled expressions of GLUT-1/3 and activities of G6PDH and 6-PGDH, thereby enhancing the transmembrane transport of glucose and metabolism of phosphopentose.

Phosphopentose metabolism can provide tumor cells with antioxidant NADPH [24, 25], maintain a high level of GSH content in tumor cells, and scavenge active oxygen free radicals generated by irradiation under the action of GSH-Px [26], which may reduce the killing effect of radiation on tumor cells to induce the radioresistance [27], that is, the changes of GSH and GSH-Px were an important pathological mechanism under stress conditions [28, 29]. Our present

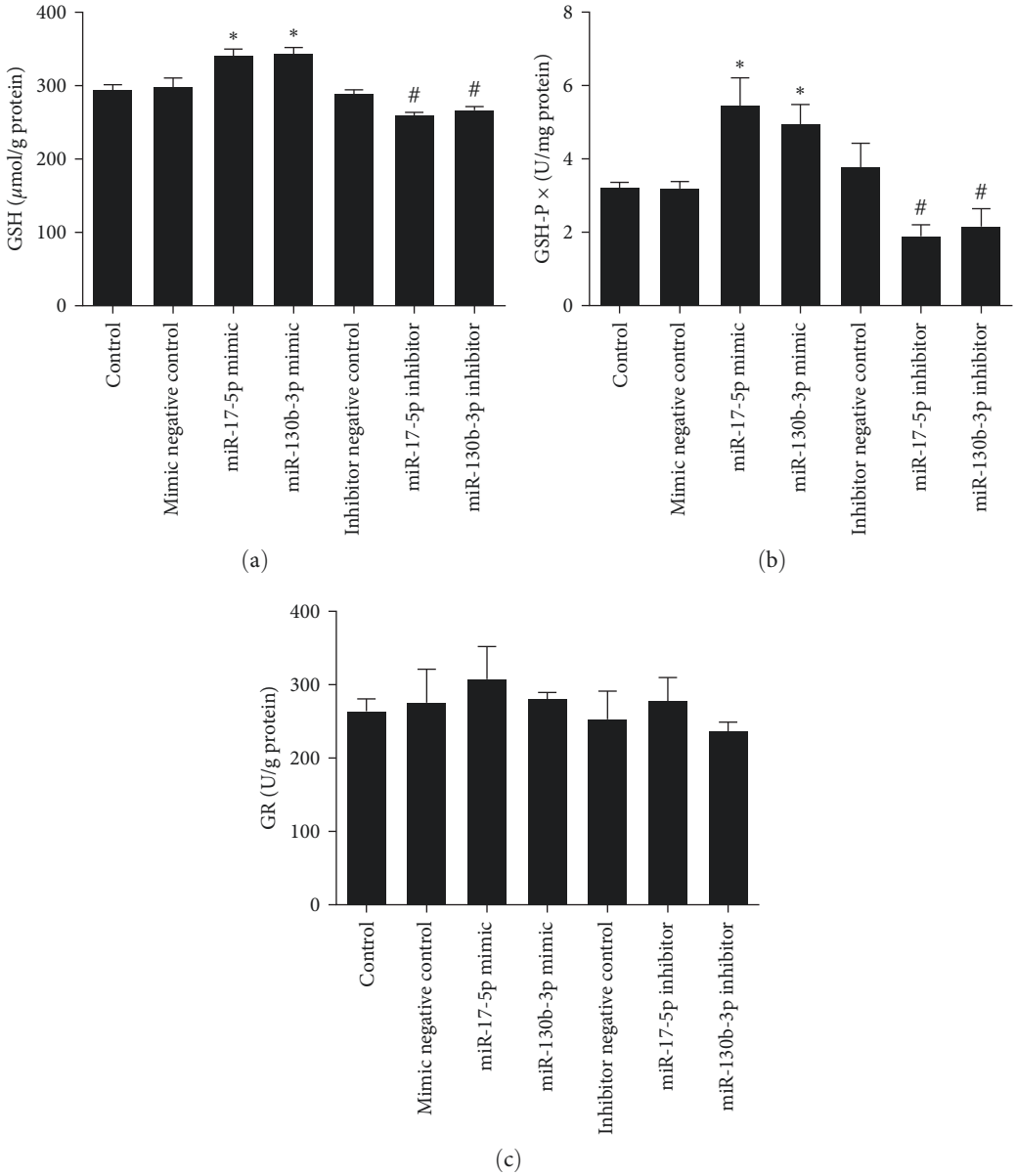

Figure 4: Intracellular GSH, GSH-Px, and GR levels after transfection of SU3 cells with miR-17-5p or miR-130b-3p mimics or inhibitors for 36 hr. Data were presented as mean ± SD of three independent experiments. $^{*}P < 0.05$ vs. the mimic negative control group; $^{\#}P < 0.05$ vs. the inhibitor negative control group.

results showed that after transfection of SU3 cells with miR-17-5p or miR-130b-3p mimics, the contents of NADPH, GSH, and GSH-Px increased substantially. On the contrary, after SU3 cells were transfected with miR-17-5p or miR-130b-3p inhibitors, the contents of NADPH, GSH, and GSH-Px decreased remarkably. These results suggested that miR-17-5p and miR-130b-3p can weaken the killing effect of radiation on tumor cells by enhancing phosphopentose metabolism and antioxidant capacity.

Bioinformatics is the main method widely used to analyze the miR target genes [30–32]. In this study, we used the miRBase and TargetScan databases and predicted the targeted binding of miR-17-5 or miR-130b-3p and PTEN 3′ noncoding regions. Further confirmation was performed using luciferase reporter gene detection. Therefore, we believed that the PTEN is a common target gene of miR-17-5p and miR-130b-3p. PTEN was closely related to the radiosensitivity of glioma cells and can negatively regulate the expression of HIF-1α by inhibiting AKT [33, 34], which is a regulatory mechanism under stress conditions [35]. Our present results showed that after SU3 cells were transfected with miR-17-5p or miR-130b-3p mimics, the expressions of PTEN mRNA and protein substantially decreased, whereas the expressions of AKT, p-AKT, and HIF-1α proteins remarkably increased. When SU3 cells were transfected with miR-17-5p or miR-130b-3p inhibitors, the opposite effects were generated. Therefore, miR-17-5p or miR-130b-3p can increase the expressions of AKT and p-AKT proteins after targeting the PTEN, which may ultimately

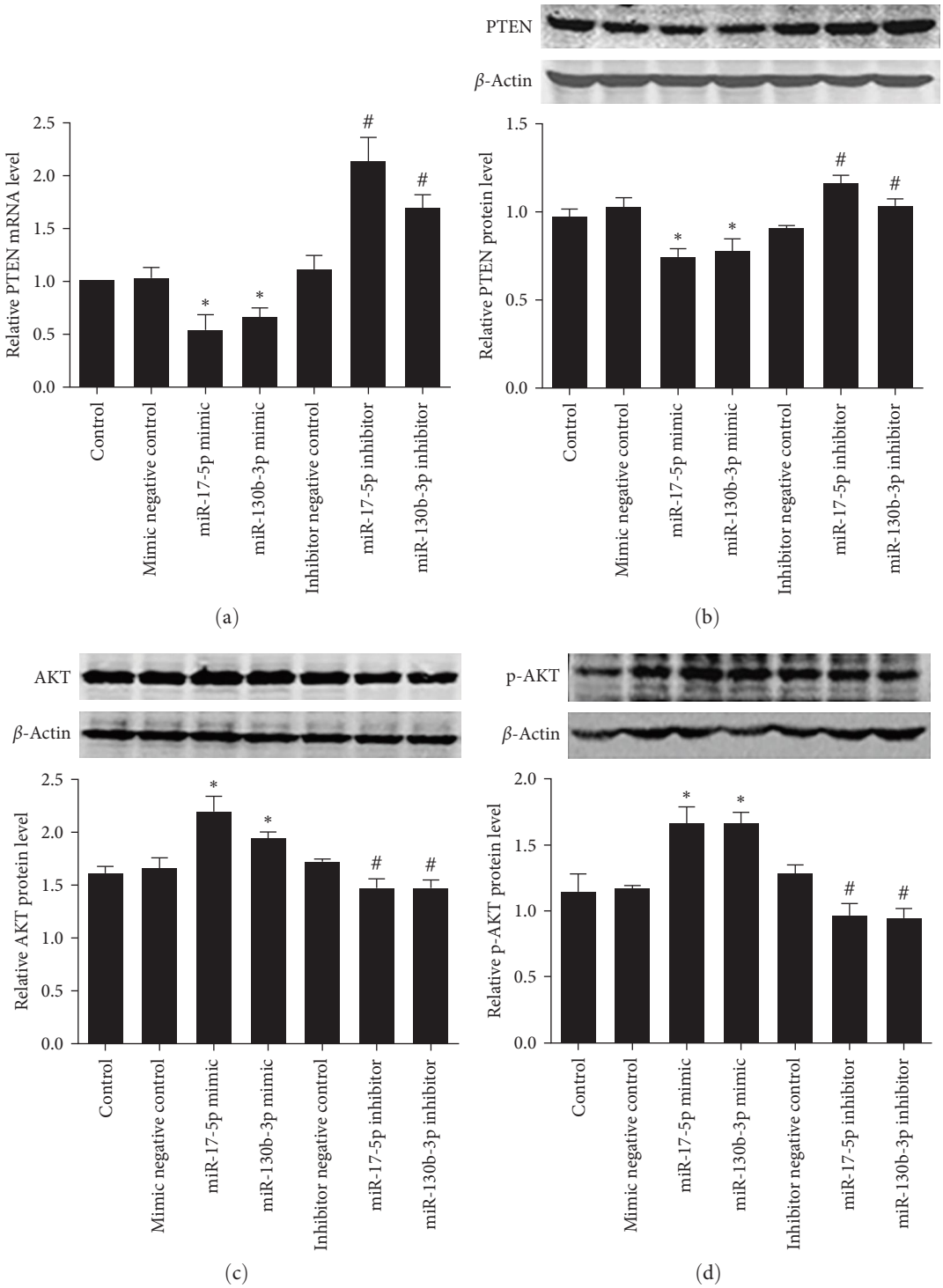

Figure 5: Continued.

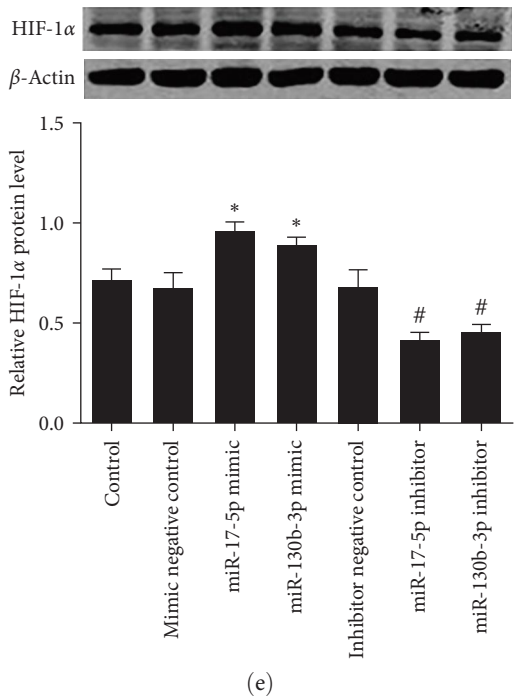

(e)

Figure 5: Intracellular PTEN, AKT, p-AKT, and HIF-1α mRNA and/or protein expressions after transfection of SU3 cells with miR-17-5p or miR-130b-3p mimics or inhibitors for 36 hr. The relative protein levels were expressed as a ratio of the densitometry of the protein of interest to that of the β-actin. Data were presented as mean $\pm$ SD of three independent experiments. $^{*}P<0.05$ vs. the mimic negative control group; $^{\#}P<0.05$ vs. the inhibitor negative control group.

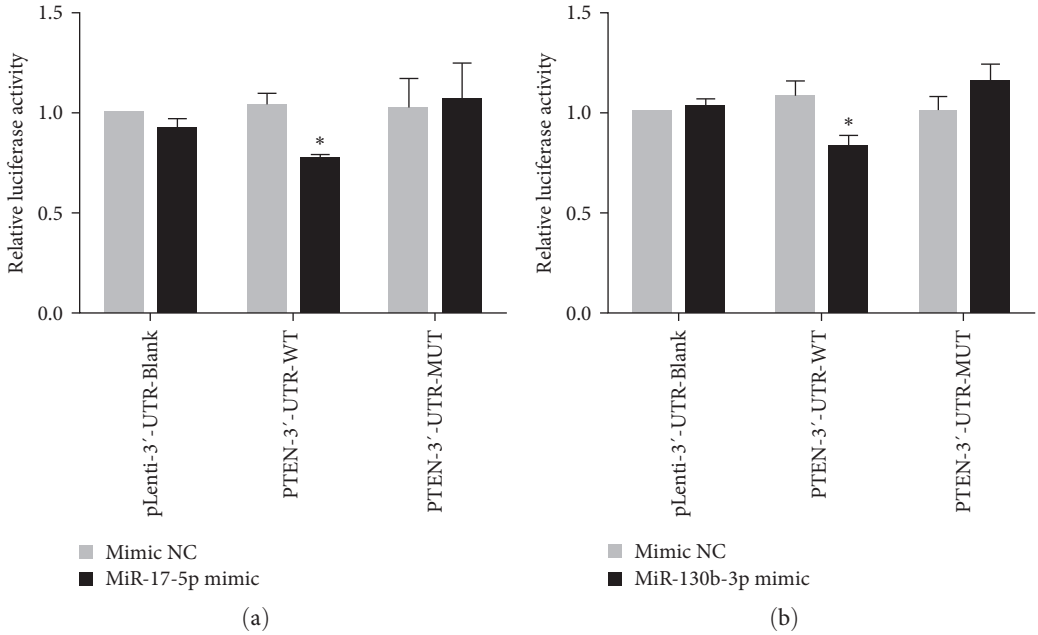

(a) (b)

Figure 6: Relative luciferase activity in SU3 cells cotransfected with PTEN 3′-UTR-WT/Mut and miR-17-5p mimic or miR-130b-3p mimic/their negative control (NC) for 48 hr. Data were presented as mean $\pm$ SD of three independent experiments. $^{*}P<0.05$ vs. the mimic NC.

result in the enhancement of HIF-1α-mediated phosphopentose metabolism and formation of radioresistance.

5. Conclusion

Our present results verified that miR-17-5p and miR-130b-3p were involved in the radioresistance of SU3 cells; the two miRs could specifically bind with the PTEN gene to weaken the negative regulatory effect of PTEN on AKT/HIF-1α signaling pathway, thereby increasing the glucose transmembrane transport, phosphopentose metabolism, and antioxidant production. These findings confirmed a radioresistant mechanism of GSCs and provided a new miR target for the study of glioma radiosensitizers.

Data Availability

The datasets used and/or analyzed during the current study are available from the corresponding authors upon reasonable request.

Conflicts of Interest

The authors declare that they have no conflicts of interest.

Authors' Contributions

T.X. and Y.H.D. performed the cell culture and treatment, western blot analysis, real-time PCR analysis, and luciferase reporter gene assay. Y.H.D. performed the measurements of cell survival rate and biochemistry indexes. T.X. analyzed the experimental data and wrote the manuscript. X.A.F. and J.D. designed the study and reviewed the manuscript. All authors approved the final manuscript. T.X. and Y.H.D. contributed equally to this work.

Acknowledgments

This work was supported by the Science & Technology Project of Suzhou City for Medical Health (LCZX201913 and KJXW2020039), the Research Fund of Nanjing Medical University (NMUB2020254), and the Research Program of Gusu School of Nanjing Medical University (GSKY20220526), China.

Supplementary Materials

Supplementary 1. Primers used in real-time PCR assay.

Supplementary 2. Sequences of predicted miR-17-5p or miR-130b-3p binding sites in PTEN 3′-UTR.

Supplementary 3. Cell viability after treatment of SU3 cells with radiation.

Supplementary 4. Intracellular miR-17-5p and miR-130b-3p expressions after incubation of SU3 or SU3-5R cells with DMEM high-glucose medium for 24 hr (A and B) or at 6, 12, and 24 hr after exposure of SU3 cells to X-ray irradiation 8 Gy (C and D).

References

[1] A. Farooqi, J. Li, J. de Groot, and D. N. Yeboa, "Current role of radiation therapy in the management of malignant central nervous system tumors," *Hematology/Oncology Clinics of North America*, vol. 34, no. 1, pp. 13–28, 2020.

[2] A. Schulz, F. Meyer, A. Dubrovska, and K. Borgmann, "Cancer stem cells and radioresistance: DNA repair and beyond," *Cancers*, vol. 11, no. 6, Article ID 862, 2019.

[3] Y. Liu, Y. Shen, T. Sun, and W. Yang, "Mechanisms regulating radiosensitivity of glioma stem cells," *Neoplasma*, vol. 64, no. 5, pp. 655–665, 2017.

[4] F. Sharifzad, S. Ghavami, J. Verdi et al., "Glioblastoma cancer stem cell biology: potential theranostic targets," *Drug Resistance Updates*, vol. 42, pp. 35–45, 2019.

[5] G. Chen, W. Zhu, D. Shi et al., "MicroRNA-181a sensitizes human malignant glioma U87MG cells to radiation by targeting Bcl-2," *Oncology Reports*, vol. 23, no. 4, pp. 997–1003, 2010.

[6] S. Xiao, Z. Yang, R. Lv et al., "MiR-135b contributes to the radioresistance by targeting GSK3 beta in human glioblastoma multiforme cells," *PLoS One*, vol. 9, no. 9, Article ID e108810, 2014.

[7] X. Han, X. Xue, H. Zhou, and G. Zhang, "A molecular view of the radioresistance of gliomas," *Oncotarget*, vol. 8, pp. 100931–100941, 2017.

[8] A. Sasaki, Y. Udaka, Y. Tsunoda et al., "Analysis of *p53* and miRNA expression after irradiation of glioblastoma cell lines," *Anticancer Research*, vol. 32, no. 11, pp. 4709–4713, 2012.

[9] W. Yu, S. Liang, and C. Zhang, "Aberrant miRNAs regulate the biological hallmarks of glioblastoma," *NeuroMolecular Medicine*, vol. 20, pp. 452–474, 2018.

[10] X. Yang, W. W. Du, H. Li et al., "Both mature miR-17-5p and passenger strand miR-17-3p target TIMP3 and induce prostate tumor growth and invasion," *Nucleic Acids Research*, vol. 41, no. 21, pp. 9688–9704, 2013.

[11] S. Lu, S. Wang, S. Geng, S. Ma, Z. Liang, and B. Jiao, "Increased expression of microRNA-17 predicts poor prognosis in human glioma," *BioMed Research International*, vol. 2012, Article ID 970761, 6 pages, 2012.

[12] M. A. Chaudhry, H. Sachdeva, and R. A. Omaruddin, "Radiation-induced microRNA modulation in glioblastoma cells differing in DNA-repair pathways," *DNA and Cell Biology*, vol. 29, no. 9, pp. 553–561, 2010.

[13] W. Hou, L. Song, Y. Zhao, Q. Liu, and S. Zhang, "Inhibition of beclin-1-mediated autophagy by microRNA-17-5p enhanced the radiosensitivity of glioma cells," *Oncology Research*, vol. 25, no. 1, pp. 43–53, 2017.

[14] J. Zhang, Y. G. Zhou, J. B. Shu et al., "MiR-130b reverses temozolomide resistance in glioma," *Chinese Journal of Pathophysiology*, vol. 35, no. 4, pp. 597–605, (Chinese), 2019.

[15] A. Wang, X. Dai, B. Cui et al., "Experimental research of host macrophage canceration induced by glioma stem progenitor cells," *Molecular Medicine Reports*, vol. 11, no. 4, pp. 2435–2442, 2015.

[16] Y. Shen, H. Chen, J. Zhang et al., "Increased notch signaling enhances radioresistance of malignant stromal cells induced by glioma stem/progenitor cells," *PLOS ONE*, vol. 10, no. 11, Article ID e0142594, 2015.

[17] F. Wang, K. Fan, Y. Zhao, and M.-L. Xie, "Apigenin attenuates TGF-β1-stimulated cardiac fibroblast differentiation and extracellular matrix production by targeting miR-155-5p/c-Ski/Smad pathway," *Journal of Ethnopharmacology*, vol. 265, Article ID 113195, 2021.

[18] X.-J. Yu, J.-C. Song, J. Du, Y.-Q. Shi, Y.-X. Liu, and Y. Shen, "GLUT-1 and its regulating factor HIF-1α expression in epithelial ovarian tumors: GLUT-1 is associated with molecular typing and grade of epithelial ovarian cancer," *International Journal of Clinical and Experimental Pathology*, vol. 10, no. 4, pp. 4479–4487, 2017.

[19] Y. Liu, Y.-M. Li, R.-F. Tian et al., "The expression and significance of HIF-1α and GLUT-3 in glioma," *Brain Research*, vol. 1304, pp. 149–154, 2009.

[20] A. Nagao, M. Kobayashi, S. Koyasu, C. C. T. Chow, and H. Harada, "HIF-1-dependent reprogramming of glucose metabolic pathway of cancer cells and its therapeutic significance," *International Journal of Molecular Sciences*, vol. 20, no. 2, Article ID 238, 2019.

[21] D. Singh, R. Arora, P. Kaur, B. Singh, R. Mannan, and S. Arora, "Overexpression of hypoxia-inducible factor and metabolic pathways: possible targets of cancer," *Cell & Bioscience*, vol. 7, Article ID 62, 2017.

[22] H. Harada, "Hypoxia-inducible factor 1-mediated characteristic features of cancer cells for tumor radioresistance," *Journal of Radiation Researh*, vol. 57, no. S1, pp. i99–i105, 2016.

[23] T. W. H. Meijer, J. H. A. M. Kaanders, P. N. Span, and J. Bussink, "Targeting hypoxia, HIF-1, and tumor glucose metabolism to improve radiotherapy efficacy," *Clinical Cancer Research*, vol. 18, no. 20, pp. 5585–5594, 2012.

[24] Y. Dong and M. Wang, "Knockdown of TKTL1 additively complements cisplatin-induced cytotoxicity in nasopharyngeal carcinoma cells by regulating the levels of NADPH and ribose-5-phosphate," *Biomedicine & Pharmacotherapy*, vol. 85, pp. 672–678, 2017.

[25] P. Jiang, W. Du, and M. Wu, "Regulation of the pentose phosphate pathway in cancer," *Protein & Cell*, vol. 5, no. 8, pp. 592–602, 2014.

[26] A. Stincone, A. Prigione, T. Cramer et al., "The return of metabolism: biochemistry and physiology of the pentose phosphate pathway," *Biological Reviews*, vol. 90, no. 3, pp. 927–963, 2015.

[27] L. Tang, F. Wei, Y. Wu et al., "Role of metabolism in cancer cell radioresistance and radiosensitization methods," *Journal of Experimental & Clinical Cancer Research*, vol. 37, Article ID 87, 2018.

[28] J. Cui, Q. Zhou, M. Yu, Y. Liu, X. Teng, and X. Gu, "4-tert-butylphenol triggers common carp hepatocytes ferroptosis via oxidative stress, iron overload, SLC7A11/GSH/GPX4 axis, and ATF4/HSPA5/GPX4 axis," *Ecotoxicology and Environmental Safety*, vol. 242, Article ID 113944, 2022.

[29] Q. Zhou, J. Cui, Y. Liu, L. Gu, X. Teng, and Y. Tang, "EGCG alleviated Mn exposure-caused carp kidney damage via trpm2-NLRP3-TNF-α-JNK pathway: oxidative stress, inflammation, and tight junction dysfunction," *Fish & Shellfish Immunology*, vol. 134, Article ID 108582, 2023.

[30] Y. Li and L. Li, "Prognostic values and prospective pathway signaling of microRNA-182 in ovarian cancer: a study based on gene expression omnibus (GEO) and bioinformatics analysis," *Journal of Ovarian Research*, vol. 12, Article ID 106, 2019.

[31] Z. Miao, Z. Miao, X. Teng, and S. Xu, "Melatonin alleviates lead-induced intestinal epithelial cell pyroptosis in the common carps (*Cyprinus carpio*) via miR-17-5p/TXNIP axis," *Fish & Shellfish Immunology*, vol. 131, pp. 127–136, 2022.

[32] J. Zhang, J. Cui, Y. Wang, X. Lin, X. Teng, and Y. Tang, "Complex molecular mechanism of ammonia-induced apoptosis in chicken peripheral blood lymphocytes: miR-27b-3p, heat shock proteins, immunosuppression, death receptor pathway, and mitochondrial pathway," *Ecotoxicology and Environmental Safety*, vol. 236, Article ID 113471, 2022.

[33] N. Inaba, M. Kimura, K. Fujioka et al., "The effect of PTEN on proliferation and drug-, and radiosensitivity in malignant glioma cells," *Anticancer Research*, vol. 31, no. 5, pp. 1653–1658, 2011.

[34] B. Xu, C. Jiang, H. Han et al., "Icaritin inhibits the invasion and epithelial-to-mesenchymal transition of glioblastoma cells by targeting EMMPRIN via PTEN/AKt/HIF-1α signaling," *Clinical and Experimental Pharmacology and Physiology*, vol. 42, no. 12, pp. 1296–1307, 2015.

[35] S. W. A. Shah, S. Zhang, M. Ishfaq, Y. Tang, and X. Teng, "PTEN/AKT/mTOR pathway involvement in autophagy, mediated by miR-99a-3p and energy metabolism in ammonia exposed chicken bursal lymphocytes," *Poultry Science*, vol. 100, no. 2, pp. 553–564, 2021.